THE JOURNAL OF BIOLOGICAL CHEMISTRY VOL. 282, NO. 52, pp. 37783–37793, December 28, 2007

Components of the Translational Machinery Are Associated with Juvenile Glycine Receptors and Are Redistributed to the Cytoskeleton upon Aging and Synaptic Activity*

Received for publication, October 5, 2007 Published, JBC Papers in Press, October 26, 2007, DOI 10.1074/jbc.M708301200

Raphael Bluem[‡1], Enrico Schmidt[‡1,2], Carsten Corvey[§], Michael Karas[§], Andrea Schlicksupp[‡], Joachim Kirsch[‡], and Jochen Kuhse[‡3]

From the [‡]Department of Anatomy and Cell Biology, University of Heidelberg, Im Neuenheimer Feld 307, 69120 Heidelberg and the [§]Department of Pharmaceutical Chemistry, University of Frankfurt, Max-von-Laue-Strasse 9, D-60438 Frankfurt, Germany

The translation eukaryotic elongation factor 1α (eEF1A) is a monomeric GTPase involved in protein synthesis. In addition, this protein is thought to participate in other cellular functions such as actin bundling, cell cycle regulation, and apoptosis. Here we show that eEF1A is associated with the α2 subunit of the inhibitory glycine receptor in pulldown experiments with rat brain extracts. Moreover, additional proteins involved in translation like ribosomal S6 protein and p70 ribosomal S6 protein kinase as well as ERK1/2 and calcineurin were identified in the same pulldown approaches. Glycine receptor activation in spinal cord neurons cultured for 1 week resulted in an increased phosphorylation of ribosomal S6 protein. Immunocytochemistry showed that eEF1A and ribosomal S6 protein are localized in the soma, dendrites, and at synapses of cultured hippocampal and spinal cord neurons. Consistent with our biochemical data, immunoreactivities of both proteins were partially overlapping with glycine receptor immunoreactivity in cultured spinal cord and hippocampal neurons. After 5 weeks in culture, eEF1A immunoreactivity was redistributed to the cytoskeleton in about 45% of neurons. Interestingly, the degree of redistribution could be increased at earlier stages of *in vitro* differentiation by inhibition of either the ERK1/2 pathway or glycine receptors and simultaneous *N*-methyl-D-aspartate receptor activation. Our findings suggest a functional coupling of eEF1A with both inhibitory and excitatory receptors, possibly involving the ERK-signaling pathway.

Inhibitory glycine receptors (GlyR)[4] and some subtypes of $GABA_A$ receptors ($GABA_AR$) in the central nervous system colocalize with gephyrin, a scaffolding protein, which is essential for the formation of densely packed receptor clusters at postsynaptic membrane specializations (1). It is believed that gephyrin-dependent cluster formation is achieved by anchoring GlyRs to the microtubular and actin-based cytoskeleton (2). In addition, gephyrin binds to collybistin (3), a guanine nucleotide exchange factor for the monomeric GTPase Cdc42 (4), and to mTOR/RAFT (5), a kinase involved in NMDA receptor-mediated signaling in the hippocampus (6).

The binding of gephyrin to the GlyR is mediated by the large cytoplasmic loop (M3M4 loop) of the GlyR β subunit (7). This polypeptide can form pentameric receptor complexes with α1, α2, and α3 subunits in spinal cord, brain stem, and cerebellum. In addition, extrasynaptic homo-oligomeric α2 receptors may exist in the developing central nervous system (8). So far it is unknown whether the homologous M3M4 loops of GlyR α subunits can also contribute binding sites for cytoplasmic proteins. Here we investigate whether the large cytoplasmic loop of the GlyR α2 subunit, which is about 37% homologous to the gephyrin-binding loop of the β subunit, can interact with cytoplasmic proteins. In pulldown experiments from brain extracts using an α2 M3M4 loop GST fusion protein, we identified eukaryotic elongation factor 1α (eEF1A), ribosomal protein S6 (rpS6), p70 S6 kinase, MAPK ERK1/2, and calcineurin as potential binding partners of GlyR α2 subunits. Consistent with these biochemical data, immunocytochemistry revealed that rpS6 and eEF1A colocalize partially with postsynaptic GlyR clusters in cultured hippocampal and spinal cord neurons. Surprisingly, in aged spinal cord neurons, eEF1A and to a lesser extend rpS6 was translocated to the microtubular cytoskeleton. The redistribution of eEF1A could be modulated by GlyR and NMDA receptor activity.

EXPERIMENTAL PROCEDURES

Plasmids

DNA fragments encoding the cytoplasmic loop sequences between transmembrane region M3 and M4 of the GlyR α2 corresponding to amino acids 342–420 of human GlyR α2 subunit (9) and the complete coding sequence of rat gephyrin (P1 clone) (10) were amplified by PCR, creating suitable flanking restriction sites. These fragments and the rat cDNA of eEF1A

* This work was supported by Deutsche Forschungsgemeinschaft Grant Ku 856/5-3 and Forschergruppe 577. The costs of publication of this article were defrayed in part by the payment of page charges. This article must therefore be hereby marked "*advertisement*" in accordance with 18 U.S.C. Section 1734 solely to indicate this fact.

[1] Both authors contributed equally to this work.

[2] Present address: BioIII, Bioinformatics and Molecular Genetics, Schaenzlestrasse 1, D-79104 Freiburg, Germany.

[3] To whom correspondence should be addressed. Tel.: 49-6221-548663; Fax: 49-6221-544952; E-mail: jochen.kuhse@urz.uni-heidelberg.de.

[4] The abbreviations used are: GlyR, glycine receptor; $GABA_A$, γ-aminobutyric acid, type A; $GABA_AR$, $GABA_A$ receptor; DIV, days *in vitro*; MALDI-TOF MS, matrix-assisted laser desorption ionization-time of flight mass spectrometry; MAP2, microtubule-associated protein 2; NMDA, *N*-methyl-D-aspartate; PBS, phosphate-buffered saline; GST, glutathione *S*-transferase; PI, phosphatidylinositol; DAPI, 4′,6-diamidino-2-phenylindole; eEF1A, eukaryotic elongation factor 1α; rpS6, ribosomal protein S6; MAPK, mitogen-activated protein kinase; ERK, extracellular signal-regulated kinase; VIAAT, vesicular inhibitory amino acid transporter; mTOR, mammalian target of rapamycin.

were cloned in the bacterial expression vector pGEX-4T1 (Amersham Biosciences) resulting in N-terminal fusion constructs with glutathione *S*-transferase (GST) (GST-α2 loop). All fusion domains were tagged at the C terminus with hexahistidyl peptide sequences.

Production and Binding of Fusion Proteins

The expression of all fusion proteins in *Escherichia coli* was performed according to the instructions of the supplier of the expression system (Amersham Biosciences). Bacterial cells of 500-ml cultures were harvested by centrifugation and resuspended in 25 ml of bacterial lysis buffer (50 mM Tris-HCl, pH 7.5, 5% glycerol, 10 mM β-mercaptoethanol, 2.5 mM $MgCl_2$, 500 mM NaCl, and EDTA-free protease inhibitor mixture (Roche Applied Science)). The cell suspensions were sonicated on ice to break the cells, and soluble proteins were obtained by centrifugation for 10 min at 10,000 $\times$ *g* at 4 °C. The supernatant was applied for binding of the GST fusion proteins on fast flow glutathione-Sepharose beads (GE Healthcare) using an Ettan-LC 900 purifier (GE Healthcare).

Pulldown Assay

Adult Wistar rat brain (1 g) was homogenized in 30 ml of tissue-lysis buffer (25 mM Tris-HCl, pH 7.5, 150 mM NaCl, 50 mM KCl, 14 mM Na_2HPO_4, 1 mM $MgCl_2$, 1 mM $CaCl_2$, 1 mM ATP, 2% (w/v) Triton, and EDTA-free protease inhibitor mixture). The homogenate was incubated at 4 °C for 1 h and centrifuged for 30 min at 4 °C with 15,000 $\times$ *g*. The column with bound GST-α2 loop fusion protein was unpacked, and the beads were incubated with 30 ml of brain extract at 4 °C by gentle agitation overnight. The column was then repacked, and the beads were washed with tissue-lysis buffer and a step gradient of 0.2 to 1 M NaCl in modified tissue-lysis buffer. Bound proteins were eluted with elution buffer (50 mM Tris-HCl, pH 8.0, 100 mM NaCl, 5 mM $MgCl_2$, and 20 mM reduced glutathione). All protein fractions from washing and the elution step (eluates) were collected and used for SDS-PAGE and immunoblotting. 60 μl of the 10$\times$ concentrated eluates were separated on 10% SDS-PAGE, and gels were stained with Coomassie Blue for detection of protein bands. For pulldown experiments using GST-eEF1A as bait, 1 g of spinal cord was used to prepare Triton X-100-solubilized protein extracts as described previously (11).

MALDI-TOF MS In-gel Digestion

Coomassie Blue-stained protein bands were excised and subjected to in-gel digestion protocols as described previously (12, 13). Peptides were extracted three times with 50% (v/v) acetonitrile in 5% (w/v) formic acid. All fractions were pooled and dried in a vacuum centrifuge prior to analysis.

Sample Preparation, Acquisition, and Interpretation of MALDI-TOF Spectra

The proteolytic digests were solved in 5 μl of 50% acetonitrile, 1% trifluoroacetic acid (v/v) (Fluka, Buchs, Switzerland). 0.5 μl of the sample was mixed with 0.5 μl of matrix (2 mg/ml 1-cyano-4-hydroxycinnamic acid (Fluka) in 50% acetonitrile, 0.5% trifluoroacetic acid) directly on a stainless steel target (PerSeptive Biosystems, Framingham, MA) and dried in ambient air. MALDI-TOF mass spectra were recorded on a Voyager-DE STR instrument (PerSeptive Biosystems). Data base searches were performed using a nonredundant data base downloaded from NCBI. In addition peptide mass fingerprint analysis was performed by a commercial analysis supplier (Toplab, Martinsried, Germany).

Cell Culture

Rat spinal cord and hippocampal neurons were prepared as described (14, 15).

Immunocytochemistry

Cultured neurons were fixed with absolute methanol at −20 °C for 10 min. Fixed cells were incubated after blocking in 1% (w/v) bovine serum albumin in PBS for 1 h with the following primary antibodies, mouse monoclonal anti-eEF1A (1:100; Upstate Biotechnology, Inc.), rabbit anti-GlyR antibody (1:100, Sigma), rabbit anti-synaptophysin (1:400; Synaptic Systems), rabbit anti-vesicular inhibitory amino acid transporter (VIAAT; 1:2000; Sigma), mouse anti-gephyrin (mAb5; 1:100), and rabbit anti-MAP2 antibody (1:2000; Chemicon). The secondary anti-mouse antibodies were conjugated to Cy3 (1:800); anti-rabbit secondary antibody was conjugated to Cy2 (1:400) or Alexa 647 (1:400). Confocal analysis was done as described (17). Analysis of fixed and labeled cells was also performed using a Zeiss Axiovert 200M motorized microscope (Zeiss, Jena, Germany) attached to a SPOT cooled CCD camera (Visitron Systems, Puchheim, Germany). All images were collected using 100$\times$ Plan-Neofluar oil objective, and digital images were analyzed using Metamorph software (Visitron Systems).

To evaluate the amount of colocalization with each receptor type or synaptic marker, we randomly selected five dendritic regions with a length of 15 μm. After setting a threshold for these regions, a quantification of the colocalization with the eEF1A immunoreactivity was determined by the software. Data analysis was done using Excel software.

Glycine-treated cells were double-stained with phospho-specific rpS6 antibody and mAb5. Settings for all image acquisitions were identical. Statistics of total pixel intensities and total cell area were calculated as mean pixel intensities using Metamorph software.

Immunohistochemistry

For immunohistochemistry a male adult Wistar rat was deeply anesthetized with diethyl ether and perfused with 4% (w/v) ice-cold phosphate-buffered paraformaldehyde. The spinal cord was post-fixed for 1 h in 4% (w/v) paraformaldehyde. The tissue was cryoprotected overnight at 4 °C in PBS with increasing sucrose concentrations (10–30% w/v) and mounted on dry ice with Tissue Tek embedding media. Spinal cord was cut at −20 °C into 20-μm cross-sections using a cryostat. The slices were rinsed three times in PBS, and the aldehyde groups were then blocked by incubation with 0.1% sodium borohydride followed two times for 10 min with 2% (w/v) H_2O_2 with 10% (w/v) methanol in PBS. The sections were permeabilized with 0.4% (w/v) Triton X-100 and blocked for 1 h in blocking buffer (1.5% (w/v) horse serum and 1% (w/v) bovine serum

albumin). Primary antibody incubation followed overnight at 4 °C in blocking buffer. Before incubation with the secondary antibody solution for 1 h at room temperature, sections were rinsed in PBS and incubated in blocking serum for 1 h. After washing the slices were mounted onto microscope slides and coverslipped (Marienfeld Lauda-Königshofen, Germany).

Pharmacological Treatment of Cultured Neurons

Treatment of Cells with Glycine—Spinal cord neurons were cultured for 6 days *in vitro* (DIV). At DIV6 cell culture medium was removed, and cells were washed once with PBS, and medium was replaced by the following salt solution: $CaCl_2$ 7 × H_2O, 207 mg/liter; KCl, 354 mg/liter; $MgSO_4$ 7 × H_2O, 160 mg/liter; $MgCl_2$ 6 × H_2O, 48.3 mg/liter; NaCl, 6.52 g/liter; $NaHCO_3$, 2.55 g/liter; NaH_2PO_4, 62.3 mg/liter; Na_2HPO_4, 62 mg/liter; KH_2PO_4, 9 mg/liter, glucose 10 mM, pH 7.4). To avoid NMDA receptor-mediated ion fluxes within cultured neurons, the salt solution was supplemented after 5 min at 37 °C with the NMDA receptor open channel blocker MK801 (10 μM). After a further 15 min of incubation at 37 °C, the salt solution was supplemented with glycine (2 mM), and cells were incubated for 5–30 min (in general 15 min) at 37 °C. In another set of experiments glycine stimulation was repeated once. Therefore, the glycine-containing solution was replaced for 15 min by salt buffer followed by an additional 15 min of glycine treatment. Wortmannin and nifedipine were used in a final concentration of 10 μM each. After treatments the salt buffer was removed, and cells were washed once with 1× PBS, and cell culture plates were put on ice. Cells from 1 well (of a 6-well plate) were scraped off with 200 μl of cell lysis buffer (250 mM Tris-HCl, pH 6.8, 4% (w/v) SDS, 1 mM sodium orthovanadate, protease inhibitor mixture (Roche Applied Science)) and treated for 5 min at 95 °C.

Treatment of Cells with NMDA, Strychnine, and ERK1/2 Inhibitor—Cultured spinal cord neurons were treated at DIV14 for 4 days by supplementing the media with 2 μM strychnine, 5 μM NMDA, 1 μM ERK1/2 inhibitor (catalog number 328006, Calbiochem), respectively, or as a combination of strychnine with NMDA or ERK1/2 inhibitor with NMDA. To identify cells with different intracellular localization of eEF1A, cells were double-labeled with rabbit antibody against VIAAT for presynaptic terminals and with anti-eEF1A antibody. For quantitative evaluation, cultures were coded, and 100 cells/treatment were selected by positive VIAAT staining. These cells were analyzed with respect to the subcellular localization of eEF1A. The number of cells with cytoskeletal localization of eEF1A was compared with control cells. The statistical analysis was made using Excel software.

Immunoblot Analysis and Statistical Analysis

Protein content was measured using 10 μl of cell lysate in 1 ml of a BCA assay (Pierce), and equal amounts of proteins were separated on NuPAGE 4–12% gels (Invitrogen). Proteins were blotted on polyvinylidene difluoride membrane (Millipore, Billerica) according to the manufacturer's instructions. Membranes were probed with mouse monoclonal eEF1A antibody (1:10,000; Upstate Biotechnology, Inc.), with rabbit phospho-rpS6 (Ser-235/236) antibody (1:4000; catalog number 2211, Cell Signaling Technology, Inc.), with rabbit phospho-rps6 (Ser-240/244) antibody (1:4000; catalog number 2215, Cell Signaling Technology, Inc.), with mouse rpS6 antibody (1:2000; catalog number 2317, Cell Signaling Technology, Inc.), with phospho-p70 S6 kinase (Thr-389) antibody (1:2000; catalog number 9205, Cell Signaling Technology, Inc.), with phospho-p70 S6 kinase (Thr-421/Ser-424) antibody (1:2000; catalog number 9204, Cell Signaling Technology, Inc.), and with a monoclonal GlyR antibody (mAb4) (1:50) (16). The horseradish peroxidase-linked secondary antibodies were detected using ECL Plus from Amersham Biosciences. After suitable exposure times films were developed and signals were scanned and analyzed using Kodak Digital Science one-dimensional software. Values of phospho-specific rpS6-signals were normalized to total rpS6-specific signals, and values are presented as relative signal intensities.

RESULTS

Identification of eEF1A and Calcineurin as Binding Partners of the GlyR α2 Subunit—To identify proteins interacting with the GlyR α2 subunit, we used a fusion protein of glutathione *S*-transferase (GST) and the large cytoplasmic loop of the GlyR α2 subunit (GST-α2 loop) as bait in pulldown experiments with rat brain extracts. GST-α2 loop or GST was expressed in *Escherichia coli*, and after extraction, GST and GST-α2 loop fusion proteins were immobilized on glutathione-Sepharose. The beads were subsequently incubated with adult rat brain extracts. After column washing, GST fusion proteins together with bound proteins were eluted with reduced glutathione, separated by SDS-PAGE, stained with Coomassie Blue, and the resulting protein patterns compared (Fig. 1*a*). Seven protein bands with apparent molecular masses ranging from 45 to 140 kDa were present in eluates of GST-α2 loop fusion protein columns but not visible in GST pulldowns and were analyzed by MALDI-TOF MS. One protein with an apparent molecular mass of about 52 kDa was identified as the translation elongation factor 1A, a monomeric GTPase involved in protein synthesis (Fig. 1*a*). Here a match of 23 peptides with a minimal coverage of 53% of the eEF1A2 sequence was found. A second protein with an apparent molecular mass of around 58 kDa (Fig. 1*a*) was identified as the Ca^{2+}-calmodulin-dependent type II phosphatase calcineurin. The other proteins identified in these experiments were LANCL1 (NCBI accession number CAB63943); eEF1Bγ (accession number 13626388); CRMP4 (accession number AAK64497); Nedd4 (accession number U50842), and nardilysin (accession number NP037125). By subsequent immunoblot analysis, LANCL, CRMP4, and Nedd4 were shown to be bound in GST pulldown experiments and therefore were excluded from further analysis. eEF1Bγ and nardilysin were not yet further analyzed. To ensure binding specificity of eEF1A and calcineurin to the GST-α2 loop fusion protein, we repeated the pulldown experiments applying higher salt washes (1 M NaCl) and included GST-gephyrin in addition to GST alone as another negative control protein. Immunoblotting experiments of protein eluates with anti-eEF1A- and anti-calcineurin-specific antibodies confirmed that both proteins bound specifically to the GST-α2 loop but not to GST alone or gephyrin-GST columns (Fig. 1, *b* and *c*). As an additional con-

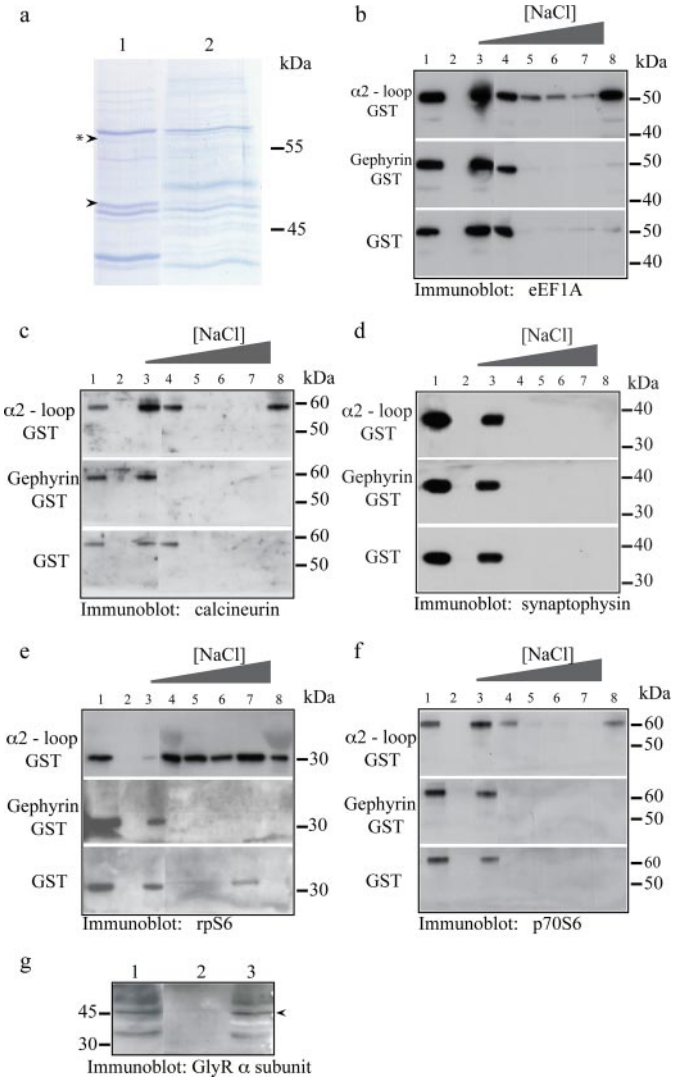

FIGURE 1. **Pulldown experiments with GST-α2 loop fusion protein and immunoblot analysis of isolated proteins.** *a,* Coomassie Blue staining of SDS-PAGE with enriched proteins of GST-α2 loop affinity chromatography experiments. Enlargement of gel-area with indication of two stained protein-bands detected in *lane 1* (GST-α2 loop) but not in *lane 2* (GST-control). Arrowhead points to eEF1A band and arrowhead with star to calcineurin. *b–f,* immunoblots of different protein fractions from pulldown experiments with immobilized GST-α2 loop fusion protein (α2 loop GST, *upper sections*), GST-gephyrin (Gephyrin GST, *middle sections*) or GST (GST, *lower sections*). All gels were loaded according to the same scheme. Brain homogenate (*lane 1*), column washing step after binding of GST-fusion proteins (*lane 2*), flow-through after loading the column with brain homogenate (*lane 3*), column washing steps with NaCl-concentration step-gradient, 0.3 M NaCl (*lane 4*), 0.4 M NaCl (*lane 5*), 0.5 M NaCl (*lane 6*), 1 M NaCl (*lane 7*) and fusion protein elution with glutathione (eluate) (*lane 8*). Using specific antibodies (*b*) eEF1A, (*c*) calcineurin, (*d*) S6 ribosomal protein (*e*) p70 S6 kinase were detected in GST-α2 eluates, but not in GST-gephyrin or GST-control experiments. *f,* synaptophysin was not detected in eluate protein fraction. *g,* isolation of GlyR subunits (*arrowhead*) with GST-eEF1A pulldown experiments. Input (*lane 1*), pulldown with GST (*lane 2*) and with GST-eEF1A fusion protein (*lane 3*) using solubilized membrane proteins from rat spinal cord.

trol we performed immunoblot analysis with GST-α2 loop pulldown experiments with rat brain extracts using an antibody directed against the presynaptic protein synaptophysin and showed that this protein did not bind to the GST-α2 loop fusion protein (Fig. 1*d*). To investigate whether the binding of eEF1A and GlyR α2 loop sequences might be direct or indirect, we cloned eEF1A1 and eEF1A2 coding sequences from rat brain cDNA into a bacterial plasmid vector allowing the expression and purification of His-tagged fusion proteins. However, using purified eEF1A1 and eEF1A2 proteins in GST-α2 loop pulldown experiments, we could not prove a direct binding of both proteins, suggesting that a bridging protein was missing in these experiments (data not shown).

Identification of Additional Components of the Translational Machinery as Binding Partners of the GlyR α2 Subunit— eEF1A is an essential component of the translational machinery. Therefore, we tested the eluted column fraction by immunoblotting for the presence of additional proteins known to be involved in regulation of protein synthesis. With this approach, we identified the rpS6 (Fig. 1*e*), which is positioned at the RNA-binding site of the 40 S small ribosomal subunit. This protein also bound to a small degree to GST alone, but could be washed off by 1 M NaCl. No rpS6 was detected in glutathione eluates from GST control experiments. The second protein identified by this approach was p70 S6 kinase, which is known to phosphorylate rpS6. Similarly, this protein was detected by immunoblotting in pulldown complexes eluted from the GST-α2 loop fusion protein but not from gephyrin-GST or GST alone (Fig. 1*f*). Again, the binding of rpS6 protein to the GST-α2 loop fusion protein was resistant to high salt washes, suggesting a high affinity binding to the GlyR α2 loop domain. To further corroborate the interaction of eEF1A with the GlyR α2 subunit, we constructed an eEF1A2-GST fusion protein expression construct and performed pulldown experiments with the purified eEF1A2-GST fusion protein and solubilized membrane proteins from rat spinal cord. These experiments revealed that eEF1A2-GST pulldown eluates contain GlyR α subunits, confirming our previous findings (Fig. 1*g*).

The Phosphorylation of rpS6 Is Modulated upon GlyR Activation—The identification of eEF1A, rpS6, and p70 S6 kinase as putative interaction partners of the GlyR suggested that the activity state of this ligand-gated ion channel might be relevant for the regulation of protein synthesis within neurons. Conceivably, the activity of p70 S6 kinase could be regulated by GlyR activity and thus the phosphorylation state of rpS6 might be dependent on GlyR activation. As rpS6 phosphorylation was shown to be one cellular mechanism for the regulation of protein synthesis (18), this scenario would have important implications for the role of GlyR activation in neurons. To further test this hypothesis we activated GlyR by increasing concentrations of glycine in cultured spinal cord neurons for a short period of time, and we subsequently analyzed the phosphorylation level of rpS6 by immunoblot experiments with cell lysates and phospho-specific antibodies directed against phosphoserine 235/236 of rpS6. For GlyR activation we replaced the culture medium by a defined buffered salt solution and supplemented the solution with 2 mM glycine. Immunoblotting of cell lysates revealed that short term glycine application resulted in increased phosphorylation of serine 235/236 of rpS6 (Fig. 2*a*). Applying glycine for different time periods (ranging from 5 to 30 min) showed that increased phosphorylation of rpS6 was first observed within 5 min after glycine application and remained at an increased level even after prolonged activation times of 30 min. These effects were blocked by preincubation with strychnine, a competitive inhibitor of glycine binding at

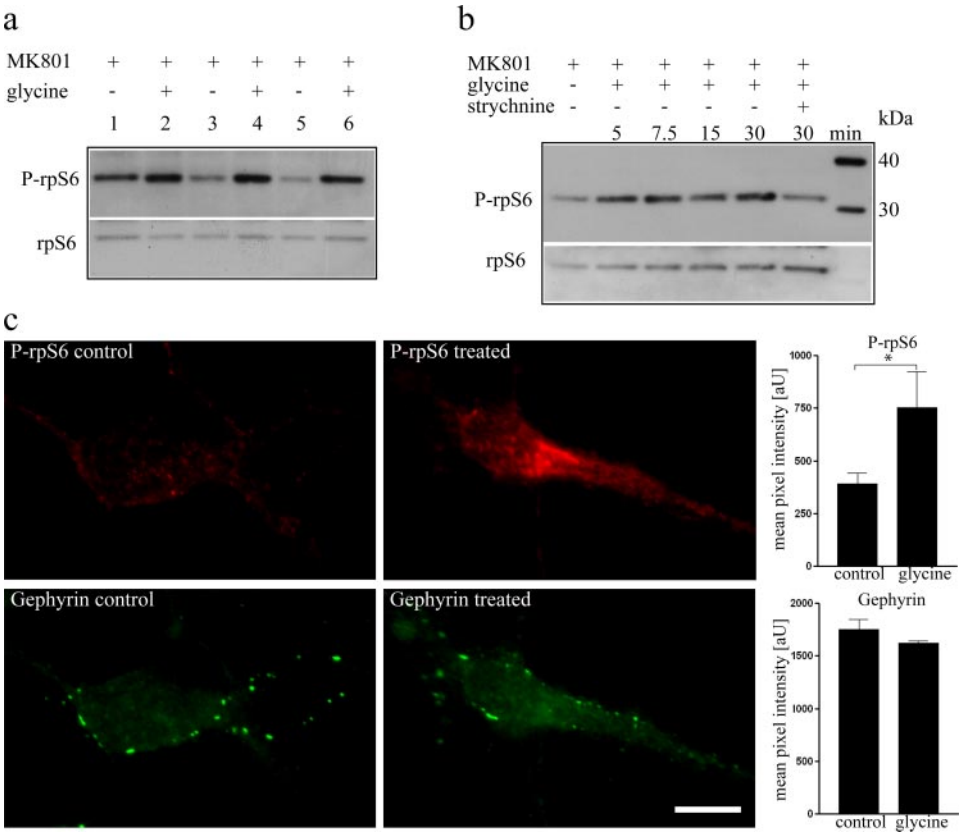

FIGURE 2. **Glycine-dependent phosphorylation of rpS6.** Glycine treatment of spinal cord neurons cultured for 6 days resulted in increased phosphorylation of rpS6 at position serine 235 and 236. *a,* phosphorylation of rpS6 was analyzed with an antibody specific for phosphorylated serines 235/236 of rpS6. Glycine treatment (2 mM) was repeated twice and led to increased phosphorylation of rpS6 (*lanes 2, 4* and *6*). *Lower panel* shows the same immunoblot probed with an antibody detecting total amount of rpS6. *b,* analysis of levels of rpS6 Ser235/236 phosphorylation in cultured spinal cord neurons treated with glycine for different time periods (5–30 min) and by glycine and strychnine (30 min, *lane 6*), a competitive inhibitor of glycine binding at GlyRs. *c,* immunofluorescence microscopy of cultured spinal cord neurons treated for 15 min with glycine using phospo-rpS6-specific antibody and quantification of mean pixel intensities (*right*). Data are expressed as mean ± S.D. of 10 cells analyzed (*, $p < 0.05$, two tailed *t* test). Note that mean pixel intensities were not changed for gephyrin immunofluorescence (*lower panel*) whereas mean pixel intensities detected for phosphorylated rpS6 were significantly increased upon glycine treatment (*upper panel*). *Bar,* 10 μm.

GlyRs (Fig. 2*b*). Cultured spinal cord neurons that were treated with glycine displayed significantly increased mean pixel intensities when probed with an antibody specific for phosphoserine 235/236 of rpS6 ($p = 0.0001$; two-tailed *t* test), whereas the mean pixel intensities using an antibody specific for gephyrin were not changed upon glycine treatment (Fig. 2*c*).

The Phosphorylation of rpS6 Is Not Dependent on the PI 3-Kinase Phosphorylation Pathway—To get further insight into possible signaling pathways involved in the glycine-dependent phosphorylation of rpS6, we analyzed the phosphorylation of p70 S6 kinase at position Thr-389, which is known to increase p70 S6 kinase activity. Immunoblot analysis with a phospho-Thr-389-specific antibody revealed that the phosphorylation of Thr-389 was not altered upon glycine application, whereas the phosphorylation of rpS6 was increased significantly ($p = 0.032$; two-tailed *t* test) under the same conditions (Fig. 3, *a* and *b*).

To further corroborate that the cellular pathway responsible for Thr-389 phosphorylation of p70 S6 kinase is indeed not involved in glycine-dependent rpS6 phosphorylation, we applied wortmannin, an inhibitor for PI 3-kinase during glycine-stimulating experiments of cultured spinal cord neurons. As shown in Fig. 3*c*, the presence of wortmannin did not result in a reduction of phosphorylated rpS6, suggesting that PI 3-kinase, an upstream kinase of mTOR, is not involved in the glycine-dependent increase of rpS6 phosphorylation (Fig. 3*c*).

It has been shown that the GlyR activation in young cultured spinal cord neurons results in depolarization rather than hyperpolarization of the postsynaptic membrane, which may induce opening of the L-type voltage-dependent Ca^{2+} channels and possibly resulting in the regulation of cellular signaling pathways (19). Therefore, we used the L-type Ca^{2+} channel blocker nifedipine to analyze whether the glycine-induced increase of rpS6 phosphorylation might be dependent on L-type channel-mediated ion fluxes. However, as shown in Fig. 3*d*, nifedipine did not inhibit the glycine-mediated increase of rpS6 phosphorylation, indicating that a yet unknown signaling pathway is involved in glycine-dependent rpS6 phosphorylation. Taken together, our results indicate that the PI 3-kinase-mTOR pathway, known to mediate NMDA receptor-dependent signaling in the hippocampus, is not responsible for GlyR-dependent cellular signaling at young stages of spinal cord neurons differentiating *in vitro*.

The MAPKs ERK1/2 are other candidate protein kinases that could be involved in rpS6 phosphorylation (20). Therefore, we reinvestigated whether ERK1/2 might also be detected as a binding protein of GlyR α2 large cytoplasmic loop by performing additional pulldown experiments using rat brain extracts. Immunoblot analysis of eluates from GST-α2 loop pulldown experiments in comparison with pulldown experiments using GST and GST-gephyrin as baits revealed that indeed ERK1/2 was present even under stringent washing conditions and could be eluted by glutathione together with the GST-α2 loop fusion protein (Fig. 4*a*). To test the putative involvement of the ERK1/2 signaling pathway in regulating glycine-dependent rpS6 phosphorylation, we stimulated cultured neurons with glycine and analyzed cell lysates using a phospho-specific antibody against MAPKs ERK1/2. These experiments revealed no significant ($p = 0.08$; two tailed *t* test) increase of MAPK activation upon glycine application (Fig. 4*b*). Furthermore, preincubation of cells with MAPK/ERK kinase inhibitors (U0126 and PD23635) did not reduce the glycine-induced increase of rpS6 phosphorylation (data not shown). These findings suggest that

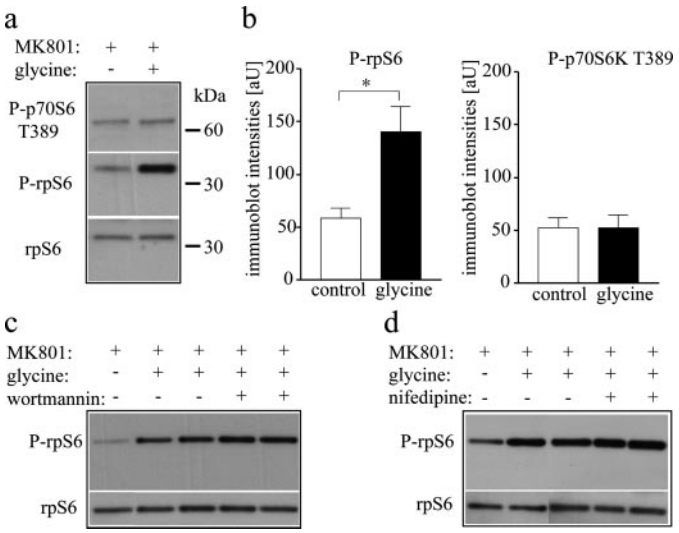

FIGURE 3. **Analysis of putative upstream kinases pathway.** Glycine-dependent increase of rpS6 Ser235/236 phosphorylation is not dependent on phosphatidylinositol 3-kinase (PI3-kinase)-mTOR/RAFT pathway. *a,* immunoblot analysis of phosphorylation of p70 S6 kinase at position threonine 389 and of rpS6 at position Ser235/236. Total rpS6 was analyzed as a loading control (*lower panel*). *b,* quantification of total pixel intensities of immunoblots shown in *a. Error bars* represent ± S.D. of at least three independent experiments (*, $p < 0.05$, two tailed *t* test). *c,* immunoblot analysis of rpS6 phosphorylation at Ser235/236 in the absence or presence of the PI3-kinase inhibitor wortmannin. Note that there is still glycine-dependent increase of rpS6 phosphorylation upon PI3-kinase inhibition. *d,* immunoblot analysis of glycine-dependent rpS6 phosphorylation in the absence or presence of the L-type Ca^{2+}-channel blocker nifedipine.

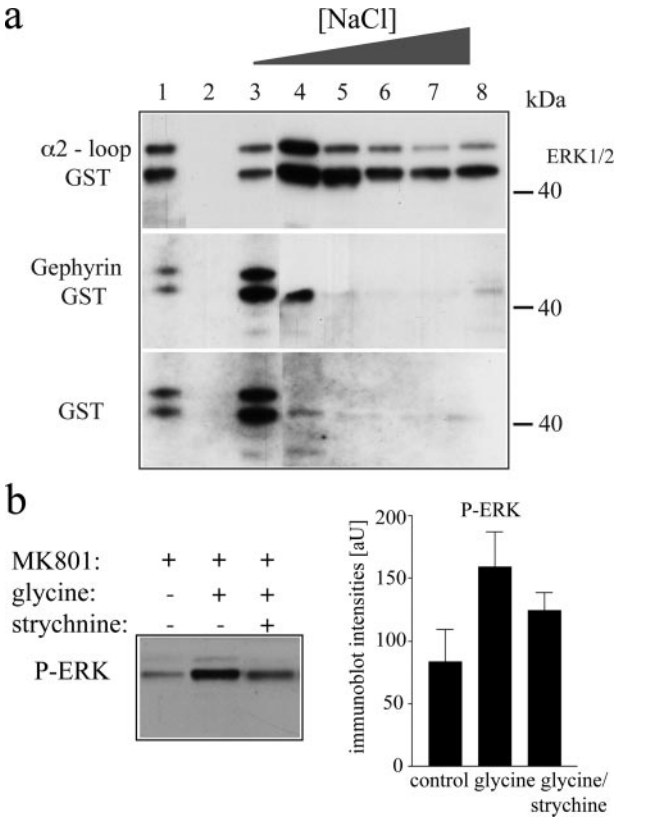

FIGURE 4. **Analysis of putative MAPK upstream pathway.** *a,* immunoblot of pulldown experiments with immobilized GST-α2 loop fusion protein (α2 loop GST, *upper sections*), GST-gephyrin (Gephyrin GST, *middle sections*) or GST (GST, *lower sections*) were probed with an antibody specific for phosphorylated MAPK (ERK1/2) protein. The loading scheme was according to Fig. 1, *b–f*. Note that phosphorylated MAPK is detected in eluted proteins (*lane 8*), whereas this protein is not detected in eluates from GST-gephyrin or GST. *b,* immunoblot analysis of protein extracts from cultures treated with glycine in the absence or presence of strychnine using an antibody specific for phosphorylated MAPK (ERK1/2) and quantification of total pixel intensities.

ERK1/2 signaling may not be involved in regulating GlyR-dependent rpS6 phosphorylation.

Subcellular Localization of rpS6 in Cultured Spinal Cord and Hippocampal Neurons—The finding that rpS6 can bind to the large cytoplasmic loop GlyR α2 subunit and that glycine-mediated activation of GlyRs in cultured spinal cord neurons resulted in increased phosphorylation of rpS6 led us to study the subcellular distributions in cultured spinal cord and hippocampal neurons by immunofluorescence microscopy. After about 1 week (DIV6), phospho-rpS6-specific immunoreactivity was found within the soma and at low levels within proximal dendrites of cultured spinal cord neurons (Fig. 5*a*). At later stages of differentiation (DIV21), phospho-rpS6 immunoreactivity within dendrites increased (Fig. 5*b*). In cultured hippocampal neurons we compared DIV8 and DIV18 stages of *in vitro* differentiation. At both stages phospho-rpS6 immunoreactivity was detected within the soma and dendrites, as described for spinal cord neurons, but in addition, immunoreactivity was found in small clusters near the cell membrane (Fig. 5, *c* and *d*). Double labeling experiments with antibodies specific for phospho-rpS6 (*green*) with either antibodies specific for VIAAT (*red*) as a marker for inhibitory presynaptic terminals (Fig. 5*e*) or gephyrin (*red*) (Fig. 5*f*) revealed that some of these spots of phospho-rpS6 are partially colocalized with the aforementioned synaptic proteins suggesting that phospho-rpS6 protein is indeed present at inhibitory synapses (Fig. 5, *e* and *f*). In addition we observed that in a small number of cells phospho-rpS6 immunoreactivity was concentrated in filamentous structures overlapping with tubulin immunoreactivity, suggesting that in these cells phospho-rpS6 is attached to microtubules (Fig. 5*g*). In addition we compared the localization of rpS6 with L7a, another ribosomal protein (large subunit) in double detection experiments at DIV21 stages of hippocampal neurons. As shown in Fig. 5*h* both antibodies detected antigens distributed throughout the dendritic compartment. However, the spatial resolution of fluorescence microscopy does not allow the determination whether these proteins are colocalized within 80 S ribosomes or not. In addition to this overall staining, L7a- and rpS6-specific immunoreactivities were also seen in separated, punctated structures (Fig. 5*h*).

Subcellular Localization of eEF1A in Cultured Spinal Cord and Hippocampal Neurons—To analyze the subcellular localization of eEF1A in neurons, we cultured hippocampal and spinal cord neurons for 1–5 weeks (DIV6 –DIV35). To determine whether eEF1A was present at synapses, we performed double labeling experiments using an eEF1A-specific antibody in combination with either anti-synaptophysin antibody as a general marker for presynaptic boutons or in combination with an antibody directed against VIAAT and a polyclonal antibody for the detection of GlyRs. As shown in Fig. 6, we identified eEF1A immunoreactivity in hippocampal neurons (DIV28) within the soma and dendrites. Small immunoreactive puncta were distributed in dendrites, and larger punctate structures apposed to

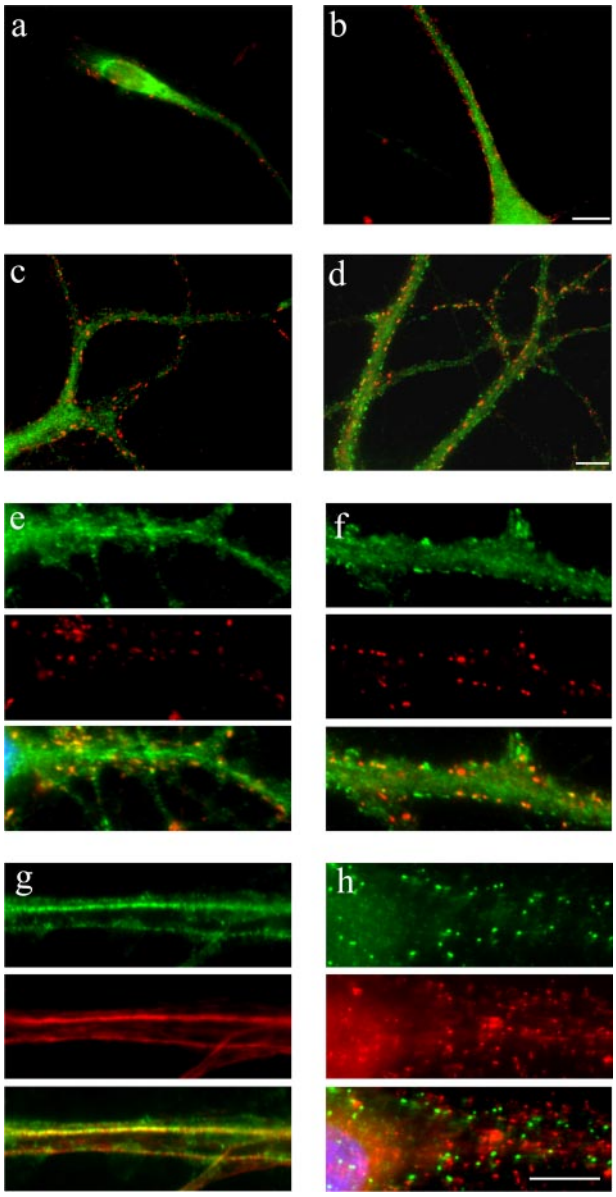

FIGURE 5. **Localization of rpS6 in cultured spinal cord and hippocampal neurons.** Spinal cord neurons were cultured for (*a*) 6 days and (*b*) 21 days and double-stained for phospho-rpS6 (*green*) and gephyrin (*red*). Hippocampal neurons were cultured for (*c*) 12 days and (*d*) 28 days and double-stained for phospho-rpS6 (*green*) and gephyrin (*red*). *e–g,* enlargements of dendritic areas from hippocampal neurons cultured for 28 days double-stained for (*e*) phospho-rpS6 (*green*) and VIAAT (*red*); *f,* phospho-rpS6 (*green*) and gephyrin (*red*); *g,* phospho-rpS6 (*green*) and tubulin (*red*) revealing a partial overlap of phospho-rpS6 with either VIAAT, gephyrin or tubulin immunoreactivities. The superimposition of *green* and *red* single channel recordings reveals in *yellow color*. *h,* rpS6 (*green*) and L7a (*red*) double staining of hippocampal neurons (DIV21). *Bars,* 10 μm.

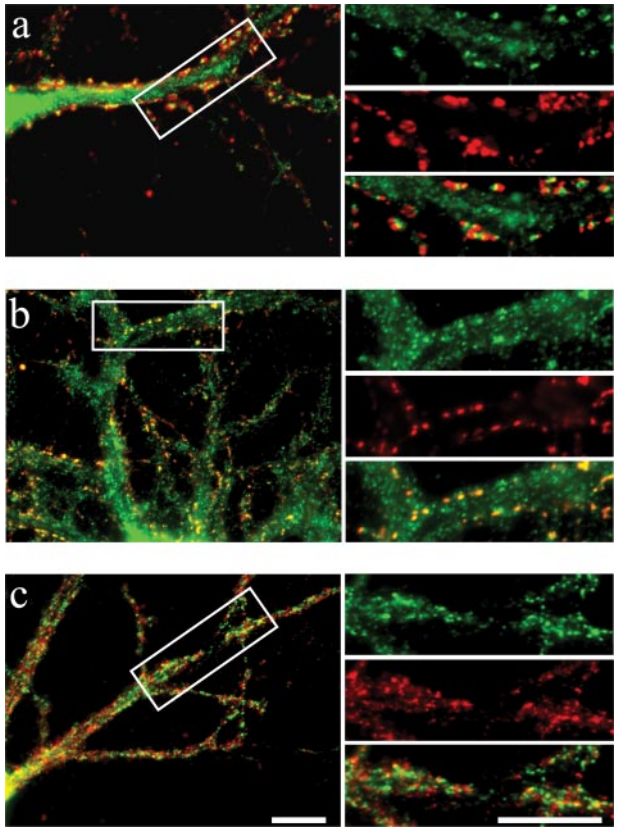

FIGURE 6. **Localization of eEF1A in cultured hippocampal neurons.** Hippocampal neurons cultured for 28 days were double-stained with antibodies directed against (*a*) eEF1A (*green*) and synaptophysin (*red*), (*b*) eEF1A (*green*) and VIAAT (*red*), (*c*) eEF1A (*green*) and GlyR (*red*). Diffuse eEF1A-immunofluorescence (*IF*) extends from the cell soma into dendrites, where a more punctuate distribution is detected (enlargements, *green color*). This IF-puncta overlap largely with punctuated synaptophysin- (66%), VIAAT- (58%) and GlyR- (49%) IFs. *Bars,* 10 μm.

presynaptic synaptophysin immunoreactivities could be seen (Fig. 6*a*). Quantification of eEF1A-specific puncta in apposition to synaptophysin revealed that the majority of eEF1A-immunoreactive puncta (66 $\pm$ 5%) was located close to synaptophysin-specific immunoreactivities (Fig. 6*a*). Double detection experiments with an eEF1A-specific and a VIAAT-specific antibody confirmed that about 58% of punctate eEF1A immunoreactivities were apposed to VIAAT-positive boutons, suggesting the localization at or near inhibitory synapses (Fig. 6*b*). Finally, we performed double detection experiments using anti-eEF1A antibody in combination with antibodies specific either for GlyRs or $GABA_A$Rs. These experiments revealed that at DIV28, about 49% of eEF1A puncta were colocalized with GlyR immunoreactivity (Fig. 6*c*), whereas only a minority of punctate eEF1A immunoreactivity colocalized with $GABA_A$Rs (data not shown). These observations suggest that specific subpopulations of inhibitory synapses might be associated with eEF1A. Similarly, we detected overlapping immunoreactivities of eEF1A with GlyR-specific immunoreactivity in cultured spinal cord neurons (DIV14–21) (data not shown), suggesting that in both types of cultured neurons a subpopulation of GlyRs carrying postsynaptic membrane specializations is associated with domains enriched in eEF1A protein.

Colocalization of eEF1A with Microtubules in Spinal Cord Neurons—In spinal cord neurons cultured for up to 4 weeks, we observed that in about 19% of the cells with VIAAT-positive boutons eEF1A immunoreactivity was not localized at synapses and dendritic puncta but instead was associated with filamentous structures within dendrites (Fig. 7*a*). This distribution was similar to the distribution of phospho-rpS6 immunofluorescence observed in some hippocampal neurons, which we had identified as microtubules. To test whether eEF1A was also associated with microtubules in these cells, we performed double detection experiments for eEF1A and MAP2. These exper-

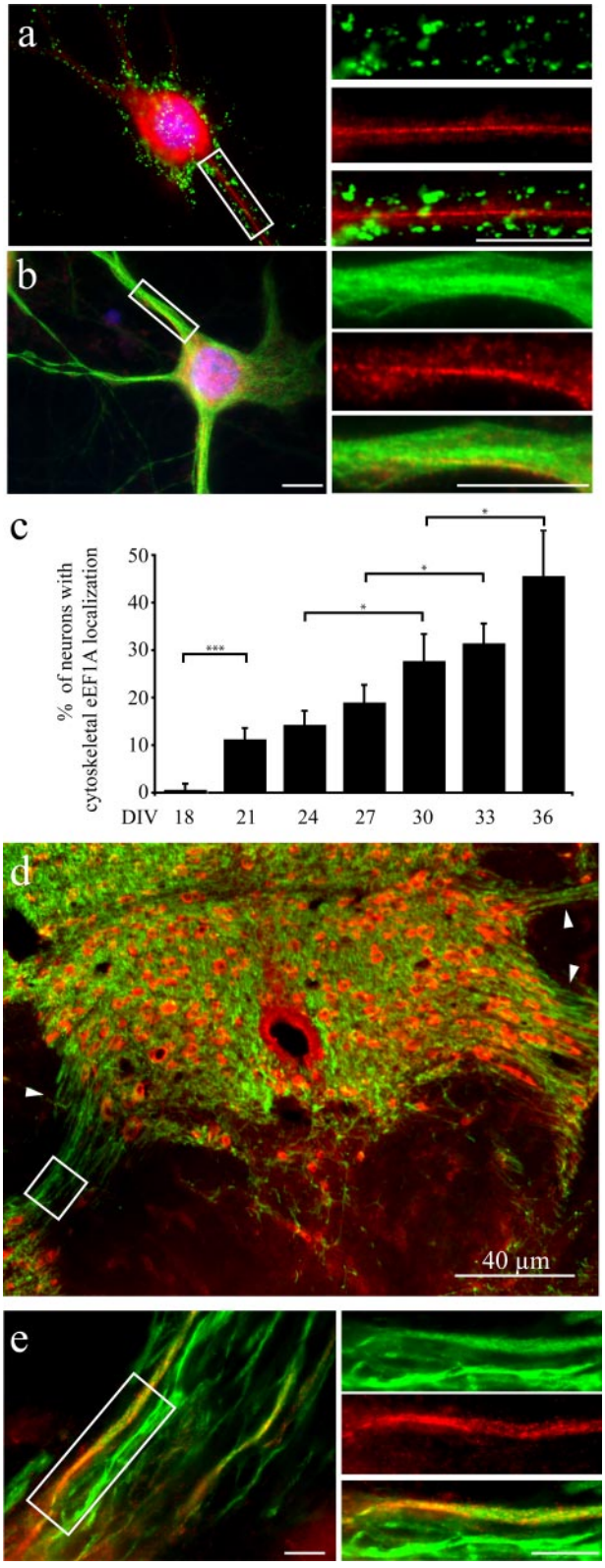

FIGURE 7. **Redistribution of eEF1A during maturation of neurons.** Spinal cord neurons were cultured for different time periods (DIV18–36) and double detection experiments of eEF1A and VIAAT were performed. *a,* in cultures from spinal cord neurons (DIV28) about 19% of neurons revealed eEF1A-IF (*red*) which was concentrated central within dendrites not overlapping with VIAAT-IF (*green*) in addition to strong somatic localization. *b,* double detection experiments with antibodies specific for MAP2 (*green*) and eEF1A (*red*) revealing an overlapping localization of both proteins (*yellow*), suggesting that eEF1A might be associated with microtubules. DAPI staining (*blue*) is shown in *a* and *b*. *c,* in spinal cord neurons cultured for longer than 18 days an increasing number of neurons displaying an altered (cytoskeletal) subcellular localization of eEF1A were evaluated. The percentage of cells with filamentous eEF1A localization within dendrites of neurons rises from 1% at DIV18 to 45% at DIV36 (*, $p < 0.05$ and ***, $p < 0.0001$, two tailed *t* test). *d,* immunohistochemical detection of eEF1A in rat spinal cord section. Double detection experiments with cranial cross-sections of spinal cord using antibodies specific for eEF1A (*red*) and MAP2 (*green*) showing partially overlaps of the IFs. *e,* magnification of boxed region in *d*. In the enlarged sector overlapping of filamentous organized eEF1A- and MAP2-IF is detectable. *Bars,* 10 μm.

iments revealed an extensive overlap of eEF1A and MAP2 immunoreactivities (Fig. 7*b*), suggesting that eEF1A is indeed associated with microtubules at DIV28 (Fig. 7*b*). Interestingly, this association with microtubules could rarely be detected in cells cultured for less than 21 days but gradually increased upon prolonged differentiation in culture, and after 5 weeks 45% of cells displayed a cytoskeletal association of eEF1A (Fig. 7*c*). Thus, our experiments revealed a redistribution of eEF1A immunoreactivities during later stages of neural differentiation. To investigate whether the redistribution of eEF1A to microtubules occurs also *in vivo*, we performed immunohistochemistry with cryosections of adult spinal cord tissue. As shown in Fig. 7*d*, we found a widespread distribution of eEF1A immunoreactivity in adult spinal cord sections. In different regions of cranial spinal cord sections, we detected filamentous eEF1A localization within extensions similar to the distribution observed at DIV28 of cultured spinal cord neurons. Double detection experiments with anti-MAP2 antibody, revealed an overlap of eEF1A-specific immunoreactivity and MAP2 immunoreactivity, suggesting that eEF1A is associated with dendritic microtubules both in cultured spinal cord neurons and *in vivo* (Fig. 7*e*, enlargement).

The Colocalization of eEF1A with Microtubules Is Dependent on the Activity of Inhibitory and Excitatory Ion Channels—To further elucidate the mechanisms of eEF1A redistribution from synapses to the cytoskeleton, we investigated whether this process might be influenced by the activity of GlyR and/or NMDA receptors. For this purpose we blocked GlyRs in cultured spinal cord neurons between DIV14 and DIV18 by supplementing the culture media with 2 μM strychnine. In additional experiments we stimulated NMDA receptors of cultured neurons for the same period of time with 5 μM NMDA, or used a combination of both ligands. After these treatments, cells were double-immunolabeled with anti-eEF1A and VIAAT antibodies. Out of 300 cells, identified by detection of VIAAT staining, the number of cells displaying filamentous eEF1A immunoreactivity was counted. We found no significant differences in the proportion of cells with eEF1A immunoreactivity at microtubules in control and strychnine-treated cells (Fig. 8*a*). A different result was obtained with cultures that had been treated with NMDA. NMDA receptor activation increased the number of neurons with eEF1A immunoreactivity at microtubules about 6-fold (Fig. 8*a*). Interestingly, a 19-fold increase of eEF1A redistribution was observed in cultures of spinal cord neurons treated with strychnine and NMDA simultaneously. Under these conditions, 19% of the cells displayed a cytoskeletal localization of eEF1A compared with 1% in untreated cultures. This observation suggests that the GlyR and NMDA receptor activity may act antagonistically on the eEF1A redistribution,

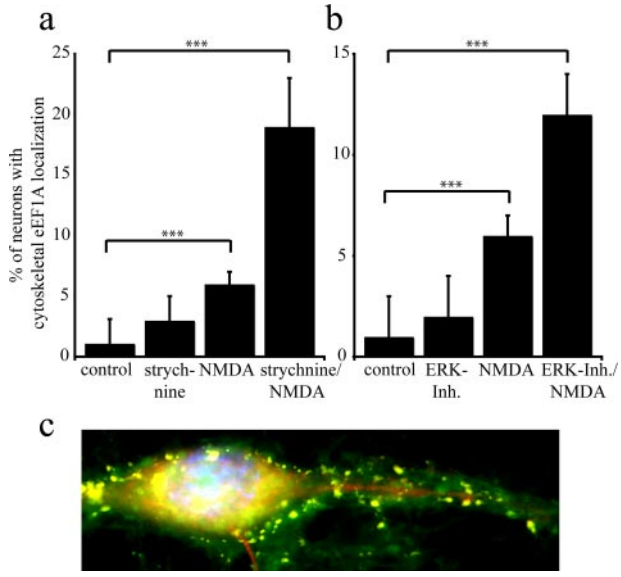

FIGURE 8. **Activity-dependent cytoskeletal localization of eEF1A.** Quantification and statistical analysis of percentage of neurons revealing a cytoskeletal association of eEF1A immunoreactivity upon (*a*) strychnine, NMDA, strychnine-NMDA treatment and (*b*) ERK1/2 inhibition, NMDA, NMDA-ERK1/2 treatment. A significant increase of the number of neurons displaying a localization of eEF1A at the cytoskeleton was seen upon NMDA receptor stimulation, by simultaneous inhibition of GlyRs and stimulation of NMDA receptors as well by ERK1/2 inhibition together with NMDA receptor activation (***, $p < 0.0001$, two tailed *t* test). *c,* immunofluorescence microscopy of cells analyzed in *a* and *b*. Calcein (*green*) and DAPI (*blue*) stainings revealed no indication of cell death of neurons with cytoskeletal eEF1A localization (*red*) upon NMDA and strychnine treatment, as the cell-permeant nonfluorescent calcein AM is only in living cells enzymatically converted into the green fluorescent calcein.

i.e. GlyR activation seems to impede whereas NMDA receptor activation stimulates eEF1A redistribution to the cytoskeleton. To exclude that NMDA and strychnine treatment induced neuronal cell death, we probed cell viability using calcein experiments and DAPI staining after 4 days of treatment with NMDA and strychnine. Treatment with both ligands did not increase the number of cells destined to cell death in our culture system (data not shown); furthermore, cells of these cultures did not reveal any indication of increased induction of apoptotic cell death (Fig. 8*c*). In addition, we treated neurons from DIV7 to DIV11 with strychnine and NMDA and analyzed eEF1A by immunofluorescence microscopy; however, no induction of redistribution was observed. In conclusion, these experiments suggest that the cytoskeletal association of eEF1A seems to be tightly correlated to age, activity, and differentiation state of cultured spinal cord neurons.

Our biochemical experiments indicate that the MAPK pathway may be involved in GlyR-dependent signaling. Therefore, we tested whether the inhibition of GlyRs by strychnine in our NMDA-strychnine treatment experiment could be mimicked by inhibition of ERK1/2 (Fig. 8*b*). Interestingly, 12% of cells revealing eEF1A redistribution to microtubules upon stimulation of NMDA receptors and simultaneous inhibition of ERK1/2 compared with about 6 or 2% with NMDA or ERK1/2 inhibitor treatment, respectively, suggesting that GlyR-dependent activation of the ERK1/2 pathway indeed might be involved in the regulation of the eEF1A redistribution to the cytoskeleton.

In conclusion, our data show that important components of the translation machinery are present at or near glycinergic synapses and that their activation status may be regulated by GlyR activation. Moreover, the ERK pathway seems to be involved in regulating the subcellular localization of eEF1A in cultured spinal cord neurons.

DISCUSSION

The elongation factor eEF1A is a GTPase, essential for the binding of aminoacyl-tRNA at the A site of the 80 S ribosome (20). In addition, several other noncanonical functions of this protein have been described. These moonlighting functions range from alterations in actin and microtubules dynamics (21, 22) to protein degradation (23), regulation of M4 muscarinic acetylcholine receptor recycling (24), apoptosis, and modulation of cellular life span (25, 26). Very recently eEF1A2, one of two isoforms expressed in vertebrates, was shown to be essential for the survival of motor neurons in mice (27).

By using a biochemical approach we demonstrate that eEF1A is a putative interaction partner of α2 subunits of GlyRs. Moreover, we demonstrate binding of two additional components of the translational machinery, namely ribosomal S6 protein and p70 S6 kinase to the GlyR α2 subunit sequence. Further biochemical experiments revealed that in young cultured spinal cord neurons GlyR activation through glycine treatment increased the phosphorylation of rpS6. In addition, we demonstrate a partial colocalization of rpS6 and eEF1A with GlyRs and also $GABA_A$Rs in the somato-dendritic compartment of cultured spinal cord and hippocampal neurons at defined stages of *in vitro* development. Therefore, it needs to be emphasized that not all of the receptor clusters colocalized with eEF1A or rpS6 immunoreactivities, respectively. These observations suggest that eEF1A and rpS6 might be associated with a defined subset of synapses, reflecting different states of activity or plasticity related processes.

For excitatory NMDA receptors, the functional role in regulating postsynaptic signaling complexes in addition to its function as ion channel is well established (28). For inhibitory receptors like GlyR and $GABA_A$Rs, the association with signaling molecules is less clear. So far, bridging proteins such as gephyrin are known to be essential for the formation of GlyR and some subtypes of $GABA_A$R clusters, probably by anchoring these receptors to the cytoskeleton. Other proteins like collybistin, a guanine exchange factor for Cdc42, was characterized as protein binding to gephyrin; however, the functional role of this interaction at synapses is unknown.

The identification of eEF1A, rpS6, and p70 S6 kinase as binding partner of the GlyR α2 subunit suggests a coupling of GlyR activity to protein synthesis. Interestingly, in *Aplysia* eEF1A was found to be involved in synaptic facilitation (29). In those experiments the long lasting phase of specific synaptic facilitation was dependent on the transport of eEF1A mRNA into the dendritic compartment and the synthesis of eEF1A next to synapses. Therefore, the authors speculated that eEF1A might be involved in determining the synapse specificity of memory storage by regulating local subsynaptic protein synthesis. Our finding that the functional coupling of the GlyR activity to phosphorylation and thus the activity state of rpS6 as one important

regulatory protein of the translational machinery supports the hypothesis that also in mammalian neurons eEF1A or other yet unknown proteins might be specifically synthesized within the dendritic compartment and that the rate of synthesis might be modulated by GlyR activity.

We demonstrate a partial colocalization of eEF1A with GlyRs in cultured spinal cord and hippocampal neurons indicating a possible functional role in synaptic plasticity. eEF1A was already identified to be present at the postsynaptic density of excitatory synapses (30); however, its functional role has not been elucidated so far. Structural proteins as tubulin and actin are known to be present at inhibitory as well as excitatory synapses (31). The identification of a protein with enzymatic activity as a shared component of inhibitory as well as excitatory synapses is novel to our knowledge.

The putative colocalization of eEF1A with actin and tubulin at both excitatory and inhibitory synapses is interesting because several studies have shown that eEF1A might be involved in the regulation of both elements of the cellular cytoskeleton. For example, it has been shown recently that dimers of *Tetrahymena piriformis*-eEF1A have Ca^{2+}-dependent actin bundling activity. Increased Ca^{2+} concentrations disrupted eEF1A dimer formation and thus led to decreased F-actin bundling, whereas low Ca^{2+} concentrations induced increased bundling activity of eEF1A (32). Thus, at excitatory synapses eEF1A might be involved in modulating plasticity processes depending on actin. Moreover, it was shown that *Xenopus* eEF1A has microtubule severing activity (33), whereas other studies revealed a microtubule binding activity for eEF1A (22). However, whether mammalian eEF1A can also fulfill these putative roles in neurons remains to be elucidated.

Interestingly, we observed a redistribution of eEF1A immunoreactivity from synapses and submembranous dendritic compartments to microtubules upon extended culture periods (3–5 weeks). In DIV7–18 cultures, only a small number (about 1%) of cells showed an association of eEF1A with the microtubular cytoskeleton. This number increased to about 45% of neurons cultured for 5 weeks. Also, rpS6 was colocalized with microtubules. Moreover, also in cranial sections from spinal cord tissue from rat, a colocalization of MAP2 immunoreactivity and staining with eEF1A-specific antibodies could be shown. To our knowledge this is the first demonstration of an association of eEF1A with microtubules *in situ* and *in vivo* in mammalian cells.

Interestingly, the redistribution of eEF1A in spinal cord neurons could be enhanced by stimulation of NMDA receptors and simultaneous blockade of GlyRs or ERK1/2 even in younger neurons. These observations are consistent with the assumption that GlyR inhibition and NMDA activation act synergistically on eEF1A redistribution. This observation also suggests that the activity-dependent redistribution of eEF1A might reflect different stages of differentiation and/or dynamic changes of synapse maturation and/or plasticity in different neurons. The model we propose is that in young neurons eEF1A is involved in protein synthesis and/or regulation of actin and microtubules dynamics in the submembranous compartment of dendrites and at subsynaptic sites. The putative regulation of actin bundling, which is well documented in several cell types (32), might be involved in the formation and maturation of postsynaptic receptor clusters or might be relevant for short distance transport processes to the membrane. In later stages of differentiation, the quantity of protein synthesis, the protein/vesicles transport, and the contribution of eEF1A to these processes might be reduced. Consequently, a redistribution of eEF1A to microtubules could stabilize these structures in mature neurons and/or might modulate transport processes along microtubules. In conclusion, we propose that GlyRs are associated with signaling molecules involved in protein synthesis and organization of the cytoskeleton. Further studies are necessary to elucidate whether the putative functions are involved in synaptic plasticity and neuronal maturation.

REFERENCES

1. Feng, G., Tintrup, H., Kirsch, J., Nichol, M. C., Kuhse, J., Betz, H., and Sanes, J. R. (1998) *Science* **282,** 1321–1324
2. Kirsch, J., and Betz, H. (1995) *J. Neurosci.* **15,** 4148–4156
3. Kins, S., Betz, H., and Kirsch, J. (2000) *Nat. Neurosci.* **3,** 22–29
4. Reid, T., Bathoorn, A., Ahmadian, M. R., and Collard, J. G. (1999) *J. Biol. Chem.* **274,** 33587–33593
5. Sabatini, D. M., Barrow, R. K., Blackshaw, S., Burnett, P. E., Lai, M. M., Field, M. E., Bahr, B. A., Kirsch, J., Betz, H., and Snyder, S. H. (1999) *Science* **284,** 1161–1164
6. Gong, R., Park, C. S., Abbassi, N. R., and Tang, S. J. (2006) *J. Biol. Chem.* **281,** 18802–18815
7. Meyer, G., Kirsch, J., Betz, H., and Langosch, D. (1995) *Neuron* **15,** 563–572
8. Hoch, W., Betz, H., and Becker, C. M. (1989) *Neuron* **3,** 339–348
9. Grenningloh, G., Schmieden, V., Schofield, P. R., Seeburg, P. H., Siddique, T., Mohandas, T. K., Becker, C. M., and Betz, H. (1990) *EMBO J.* **9,** 771–776
10. Prior, P., Schmitt, B., Grenningloh, G., Pribilla, I., Multhaup, G., Beyreuther, K., Maulet, Y., Werner, P., Langosch, D., Kirsch, J., and Betz, H. (1992) *Neuron* **8,** 1161–1170
11. Pfeiffer, F., and Betz, H. (1981) *Brain Res.* **226,** 273–279
12. Rosenfeld, J., Capdevielle, J., Guillemot, J. C., and Ferrara, P. (1992) *Anal. Biochem.* **203,** 173–179
13. Shevchenko, A., Jensen, O. N., Podtelejnikov, A. V., Sagliocco, F., Wilm, M., Vorm, O., Mortensen, P., Boucherie, H., and Mann, M. (1996) *Proc. Natl. Acad. Sci. U. S. A.* **93,** 14440–14445
14. Kirsch, J., Wolters, I., Triller, A., and Betz, H. (1993) *Nature* **366,** 745–748
15. Dresbach, T., Hempelmann, A., Spilker, C., tom Dieck, S., Altrock, W. D., Zuschratter, W., Garner, C. C., and Gundelfinger, E. D. (2003) *Mol. Cell. Neurosci.* **23,** 279–291
16. Pfeiffer, F., Simler, R., Grenningloh, G., and Betz, H. (1984) *Proc. Natl. Acad. Sci. U. S. A.* **81,** 7224–7227
17. Pauly, T., Schlicksupp, A., Neugebauer, R., and Kuhse, J. (2005) *Neuroscience* **131,** 99–111
18. Bader, A. G., Kang, S., Zhao, Li., and Vogt, P. K. (2005) *Nat. Rev. Cancer* **5,** 921–929
19. Yoshida, M., Fukuda, S., Tozuka, Y., Miyamoto, Y., and Hisatsune, T. (2004) *J. Neurobiol.* **60,** 166–175
20. Hong-Brown, L. Q., Brown, C. R., and Lang, C. H. (2004) *Am. J. Physiol.* **287,** 482–492
21. Gross, S. R., and Kinzy, T. G. (2005) *Nat. Struct. Mol. Biol.* **12,** 772–778
22. Moore, R. C., and Cyr, R. J. (2000) *Cell Motil. Cytoskeleton* **45,** 279–292
23. Chuang, S. M., Chen, L., Lambertson, D., Anand, M., Kinzy, T. G., and Madura, K. (2005) *Mol. Cell. Biol.* **25,** 403–413
24. McClatchy, D. B., Fang, G., and Levey, A. I. (2006) *Neurochem. Res.* **31,** 975–988
25. Ruest, L. B., Marcotte, R., and Wang, E. (2001) *J. Biol. Chem.* **277,** 5418–5425
26. Shepherd, J. C., Walldorf, U., Hug, P., and Gehring, W. J. (1989) *Proc. Natl. Acad. Sci. U. S. A.* **86,** 7520–7521

27. Newbery, H. J., Loh, D. H., O'Donoghue, J. E., Tomlinson, V. A., Chau, Y. Y., Boyd, J. A., Bergmann, J. H., Brownstein, D., and Abbott, C. M. (2007) *J. Biol. Chem.* **282,** 28951–28959
28. Blackstone, C., and Sheng, M. (1999) *Cell Calcium* **26,** 181–192
29. Giustetto, M., Hegde, A. N., Si, K., Casadio, A., Inokuchi, K., Pei, W., Kandel, E. R., and Schwartz, J. H. (2003) *Proc. Natl. Acad. Sci. U. S. A.* **100,** 13680–13685
30. Cho, S. J., Jung, J. S., Ko, B. H., Jin, I., and Moon, I. S. (2004) *Neurosci. Lett.* **366,** 29–33
31. Kelly, P. T., and Cotman, C. W. (1978) *J. Cell Biol.* **79,** 173–183
32. Bunai, F., Ando, K., Ueno, H., and Numata, O. (2006) *J. Biochem.* (*Tokyo*) **140,** 393–399
33. Shiina, N., Gotoh, Y., Kubomura, N., Iwamatsu, A., and Nishida, E. (1995) *Science* **266,** 282–285